

1 Supplementary Information

2

3 **Weathering Pathways Differentially Affect Colloidal Stability of**
4 **Nanoplastics**

5 Tianchi Cao, Mengting Zhao, Tong Zhang* and Wei Chen

6

7

8 College of Environmental Science and Engineering, Ministry of Education Key Laboratory of
9 Pollution Processes and Environmental Criteria, Tianjin Key Laboratory of Environmental
10 Remediation and Pollution Control, Nankai University, Tianjin 300350, China

11

12

13

14

15

16

17

18

19

20

21

22 * Corresponding authors: (E-mail) zhangtong@nankai.edu.cn

23

24 Manuscript prepared for *Environmental Science: Nano*

25

26

Number of pages: 13

27

Number of tables: 1

28

Number of figures: 5

29

1 **1. MATERIALS AND METHODS**

2 **1.1 Materials and Chemicals**

3 The aqueous suspension of pristine polystyrene (PS) nanoplastics ($25 \text{ g}\cdot\text{L}^{-1}$) was purchased
4 from Tianjin Junyijia Technology Co., Ltd. According to the supplier, the PS nanoplastics have
5 an approximate diameter of 100 nm. To remove any potential additives and surfactants, such
6 as sodium dodecyl sulfate (SDS), the PS nanoplastics were centrifuged at 40,000 rpm for 40
7 minutes (Optima XE-100, Beckman, USA). The supernatant was carefully discarded, and the
8 pellet was washed with deionized water. This centrifugation and rinsing procedure was
9 repeated five times. Following the centrifugation and rinsing process, the PS nanoplastics were
10 diluted to a final concentration of $10 \text{ g}\cdot\text{L}^{-1}$ using deionized water. The prepared PS nanoplastic
11 suspension was then stored in brown glass bottles at 4°C for future use.

12 $\text{Na}_2\text{S}\cdot 9\text{H}_2\text{O}$, NaNO_3 , and $\text{NH}_3\cdot\text{H}_2\text{O}$ (25 % w/v in H_2O) were purchased from Aladdin
13 Biological Technology (Shanghai, China). NaCl , NaOH , HCl , and CaCl_2 were obtained from
14 Sigma-Aldrich. Suwannee River Humic Acid (SRHA, Standard III, 3S101H) and Suwannee
15 River Fulvic Acid (SRFA, Standard III, 3S101F) were supplied by the International Humic
16 Substances Society. The total organic carbon (TOC) content of SRHA and SRFA was
17 determined using a TOC analyzer (Shimadzu, Japan).

18 **1.2 Sulfide- and UV-induced aging experiments**

19 To closely replicate the environmental conditions that nanoplastics experience in real-world
20 environments, well-established weathering treatments (e.g., sulfide- and UV-aging) were
21 chosen to achieve a representative degree of aging comparable to naturally weathered
22 nanoplastics.^{1, 2} For sulfide-induced aging treatment, a specific volume of stock polystyrene
23 (PS) nanoplastic suspension was added to a Tris buffer solution (10 mM, pre-adjusted to neutral
24 pH) to obtain a final PS nanoplastic concentration of 10 mg/L. This suspension was purged
25 with nitrogen (N_2) for at least 30 minutes to create an oxygen-deficient environment.
26 Immediately before use, a sulfide stock solution was prepared by dissolving $\text{Na}_2\text{S}\cdot 9\text{H}_2\text{O}$ in the
27 Tris buffer. This sulfide solution was added to the PS suspension to achieve a Na_2S
28 concentration of 0.1 mM. The reactor was then sealed with minimal headspace and placed on

1 an orbital shaker at 160 rpm and 25 °C in the dark for 7 days. After the sulfide treatment period,
2 the suspension of PS nanoplastics was centrifuged using an Optima XE-100 (Beckman, USA)
3 and rinsed with deionized water five times to eliminate any residual $\text{Na}_2\text{S}\cdot 9\text{H}_2\text{O}$. Each
4 centrifugation cycle was conducted at 40,000 rpm for 40 minutes. The cleaned PS nanoplastics
5 were then diluted to a final concentration of $10 \text{ g}\cdot\text{L}^{-1}$ using deionized water and sonicated to
6 ensure even dispersion. The prepared sulfide-aged PS nanoplastics suspension was
7 subsequently stored in brown glass bottles at 4 °C for future experiments. The samples that
8 underwent sulfide treatment are designated as PS-S.

9 For UV-induced aging treatment, a specific amount of the PS stock suspension was added
10 to a sodium nitrate (NaNO_3) solution to achieve a final concentration of $0.2 \text{ g}\cdot\text{L}^{-1}$ PS
11 nanoplastics and 5 mM NaNO_3 . The resulting PS nanoplastics suspension was transferred to a
12 50 mL quartz photoreaction tube. The tube was placed in a photochemical reaction apparatus
13 (XPA-7, Xujiang Electromechanical Plant, Nanjing, China) and irradiated with a 500 W
14 mercury lamp (UVA, wavelength 365 nm) for 6 hours at a temperature of 25°C, with
15 continuous stirring using the internal magnetic stirrer to ensure thorough mixing. Following
16 UV irradiation, the suspension of PS nanoplastics was processed through centrifugation and
17 rinsing steps similar to those described earlier for PS-S mentioned. The resulting UV-aged PS
18 nanoplastics stock suspension ($10 \text{ g}\cdot\text{L}^{-1}$) was also transferred to brown glass bottles and stored
19 at 4 °C for future use. The samples treated with UV irradiation are referred to as PS-UV.

20 **1.3 Characterization of nanoplastics**

21 The physical dimensions and morphologies of the pristine, sulfide-aged, and UV-aged
22 nanoplastics were characterized with scanning electron microscopy (SEM, S-3400 N II,
23 Hitachi, Japan) and transmission electron microscope (TEM, JEM-2100, JEOL, Japan). The
24 particle size and its distribution were determined using ImageJ software by analyzing at least
25 200 particles in the SEM images of nanoplastics. The functional groups and chemical
26 composition of nanoplastics were analyzed by Fourier transform infrared spectroscopy (FTIR,
27 TENSOR 37, Bruker, Germany) and X-ray photoelectron spectroscopy (XPS, PHI 5000
28 VersaProbe, Tokyo, Japan). The relative surface hydrophobicity of nanoplastics was evaluated
29 by measuring the contact angle (OCA-20, Dataphysics Instruments GmbH, Germany). The zeta

1 potential of nanoplastics over a range of electrolyte concentrations and pH were determined
2 using a Litesizer 500 instrument (Anton Paar).

3 **1.4 Aggregation kinetics of PS nanoplastics**

4 Time-resolved dynamic light scattering (DLS, Litesizer 500 instrument, Anton Paar) was
5 employed to measure the increase in average hydrodynamic diameter (D_h) of PS nanoplastics
6 as a function of time under different solution chemistries at a temperature of 25 °C. All the
7 solutions (including PS nanoplastics suspension, deionized water, and electrolyte solution)
8 were adjusted to the same pH condition before test. Several pH conditions (pH 5, pH 7, and pH
9 9) were chosen to study the effect of initial pH on nanoplastics aggregation. The remaining
10 experiments were conducted at a pH of 6. The concentration of PS nanoplastics was selected
11 to be 10 mg/L, a level reported in several prior studies and considered environmentally relevant
12 as it may be found in contaminated natural water systems. For each aggregation experiment,
13 0.5 mL of a 30 mg/L PS nanoplastics suspension was added to a pre-cleaned disposable
14 polystyrene cuvette. Specific volumes of deionized water and electrolyte solution were then
15 added to achieve a total solution volume of 1.5 mL with the desired electrolyte concentration.
16 The cuvette was briefly vortexed for several seconds before being promptly placed into the
17 chamber of the dynamic light scattering (DLS) instrument to commence measurement. The
18 hydrodynamic diameter of the PS nanoplastics was recorded, with the autocorrelation function
19 collected over a period of 20 seconds. Each aggregation experiment was conducted for up to
20 60 minutes, during which a significant increase in D_h was observed. The apparent aggregation
21 rate coefficient (k_{app}) was determined from the increase in the D_h as follows:

$$k_{app} = \frac{1}{D_h(0)} \left(\frac{dD_h(t)}{dt} \right)_{t \rightarrow 0} \quad (S1)$$

22 Where t represents the experimental time and $D_h(0)$ is the hydrodynamic radius of the PS
23 nanoplastics in a stable suspension. The aggregation kinetics of PS nanoplastics under various

1 salt solution conditions were quantified by calculating the attachment efficiency (α) using the
 2 following equation:

$$\alpha = \frac{k_{app}}{k_{app(fast)}} \quad (\text{S2})$$

3 where the subscript “fast” denotes fast or diffusion-controlled aggregation of nanoplastics,
 4 which was achieved at high NaCl concentrations (e.g., 600 and 1000 mM). An attachment
 5 efficiency value close to unity signifies that the system is unstable and the nanoplastics undergo
 6 rapid aggregation. In contrast, smaller attachment efficiency values indicate a more stable
 7 system with slower particle aggregation.

8 The attachment efficiencies (α) for PS nanoplastics in NaCl solutions can be predicted
 9 based on the classic Derjaguin-Landau-Verwey-Overbeek (DLVO) theory using following
 10 equation for two identical sphere-sphere interactions:

$$\alpha = \frac{\int_0^{\infty} \beta(h) \frac{\exp[-V_T(h)/k_B T]}{(2R+h)^2} dh}{\int_0^{\infty} \beta(h) \frac{\exp[-V_A(h)/k_B T]}{(2R+h)^2} dh} \quad (\text{S3})$$

11 where h represents the separation distance between the surfaces of two particle, k_B is the
 12 Boltzmann constant, T is the absolute temperature, R is the initial radius of particles in the
 13 suspension, which is assumed as the measured hydrodynamic radius, and $\beta(h)$ is a
 14 dimensionless function that corrects the hydrodynamic interactions between two approaching
 15 particles. According to the classic DLVO theory, $V_T(h)$ is the total interaction energy between
 16 two particles, which is the sum of the van der Waals attraction, $V_A(h)$, and electrical double
 17 layer repulsion, $V_R(h)$:

$$V_T(h) = V_A(h) + V_R(h) \quad (\text{S4})$$

$$\beta(h) = \frac{6\left(\frac{h}{R}\right)^2 + 13\left(\frac{h}{R}\right) + 2}{6\left(\frac{h}{R}\right)^2 + 4\left(\frac{h}{R}\right)} \quad (\text{S5})$$

1 The van der Waals attraction, $V_A(h)$, was calculated using Gregory's expression which
2 considers the electromagnetic retardation effect:

$$V_A(h) = -\frac{HR}{12h} \left[1 - \frac{bh}{\lambda} \ln \left(1 + \frac{bh}{\lambda} \right) \right] \quad (\text{S6})$$

3 where H is the Hamaker constant between the interacting PS nanoplastics in aqueous medium
4 (J), R and h retain their previously defined meanings, b is equal to 5.32, λ represents the
5 "characteristic wavelength" of the interaction, commonly assumed to be approximately 100
6 nm.

7 The electrical double layer repulsion, $V_R(h)$, can be calculated using three common
8 methods: constant charge approximation (CCA), linear superposition approximation (LSA),
9 and constant potential approximation expressions. In this study, the LSA expression was
10 employed because it produces intermediate results between the extreme assumptions of
11 constant surface charge and constant surface potential. The LSA expression is given by:

$$V_R(h) = -\frac{64\pi R n_\infty k_B T}{\kappa^2} \gamma^2 \exp(-\kappa h) \quad (\text{S7})$$

12 where the bulk number density of ions, the inverse Debye length κ (m^{-1}), and γ are given by:

$$n_\infty = 1000 N_A C_s \quad (\text{S8})$$

$$\kappa = 2.32 \times 10^9 \left(\sum c_i z_i^2 \right)^{\frac{1}{2}} \quad (\text{S9})$$

$$\gamma = \tanh \left(\frac{ze\varphi}{4k_B T} \right) \quad (\text{S10})$$

13 where N_A is the Avogadro number ($6.02 \times 10^{23} \text{ mol}^{-1}$), C_s is the electrolyte molar concentration
14 (mol L^{-1}), z_i denotes the valence of the ion i , e is the electron charge ($-1.60 \times 10^{-19} \text{ C}$), and φ is

1 the surface potential of PS nanoplastics (V), which is approximated by zeta potential.

2

3

Table S1 Surface chemical compositions of PS, PS-UV, and PS-S nanoplastics obtained from XPS spectra.

NPs	Total C (%)	Total O (%)	Total S (%)	O/C (%)	C-C/C=C (%)	C-O (%)	C=O (%)
PS	95.91	3.92	0.17	0.04	97.90	2.10	0
PS-UV	85.70	14.12	0.18	0.16	86.26	7.45	6.29
PS-S	92.07	7.64	0.29	0.08	90.28	7.80	1.91

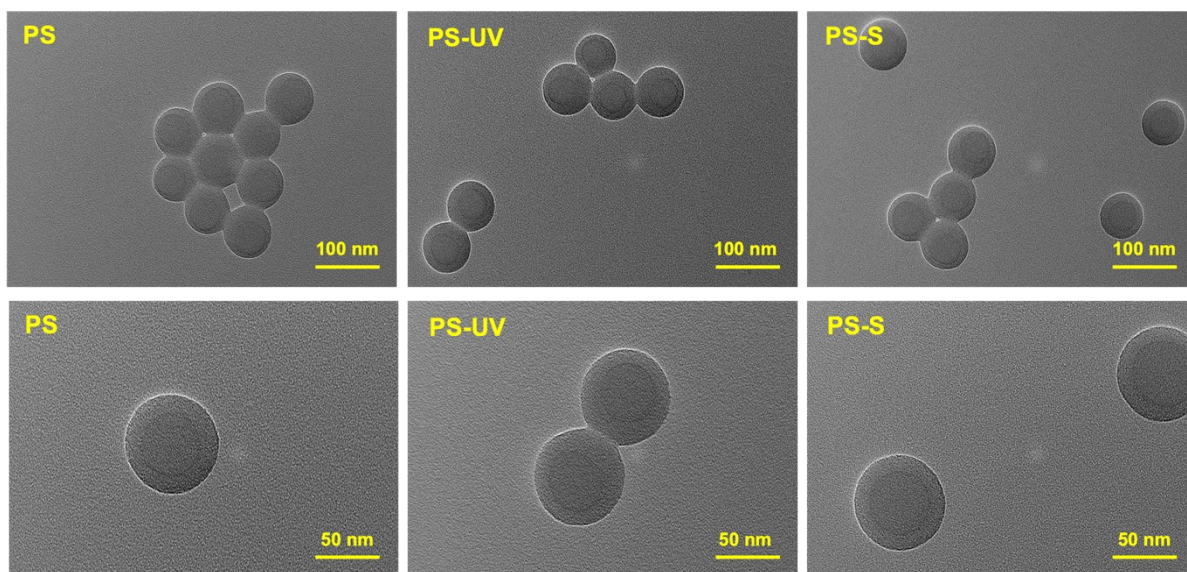


Fig. S1. TEM images of PS, PS-UV, and PS-S nanoplastics

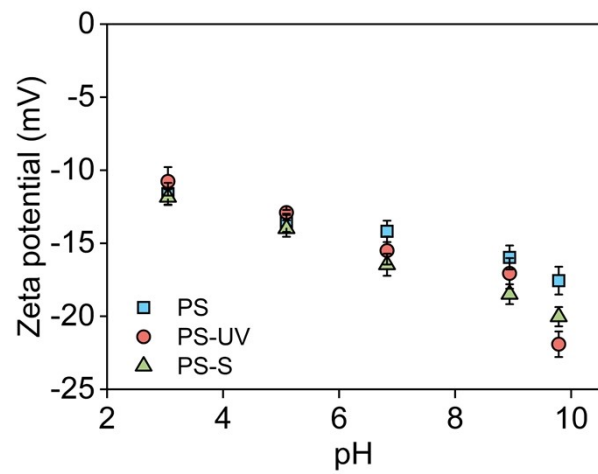


Fig. S2. Zeta potential of PS, PS-UV, and PS-S nanoplastics under different pH conditions in deionized water.

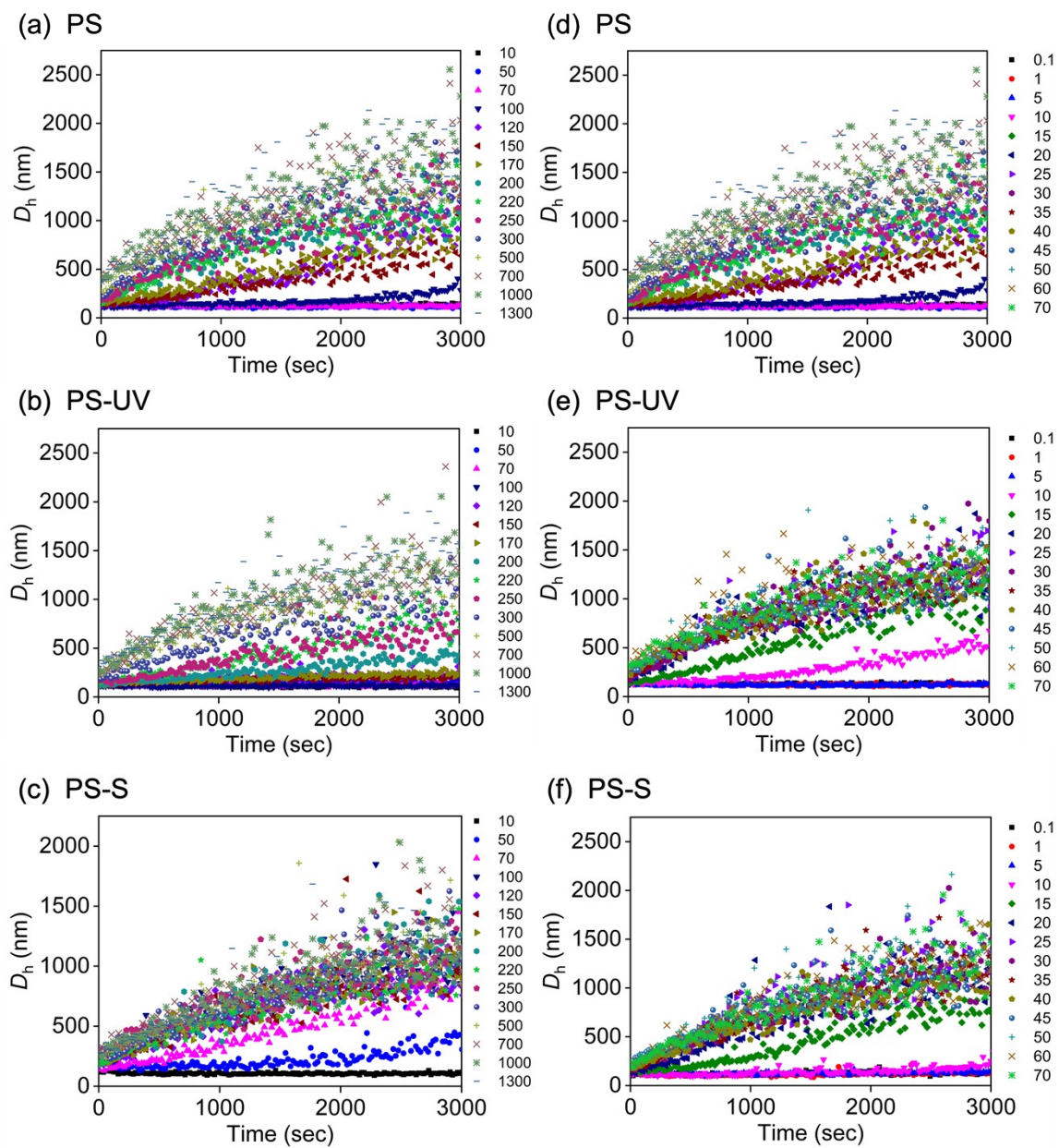


Fig. S3. Aggregation kinetics of PS, PS-UV, and PS-S nanoplastics at different NaCl (a-c) and CaCl₂ (d-f) concentrations.

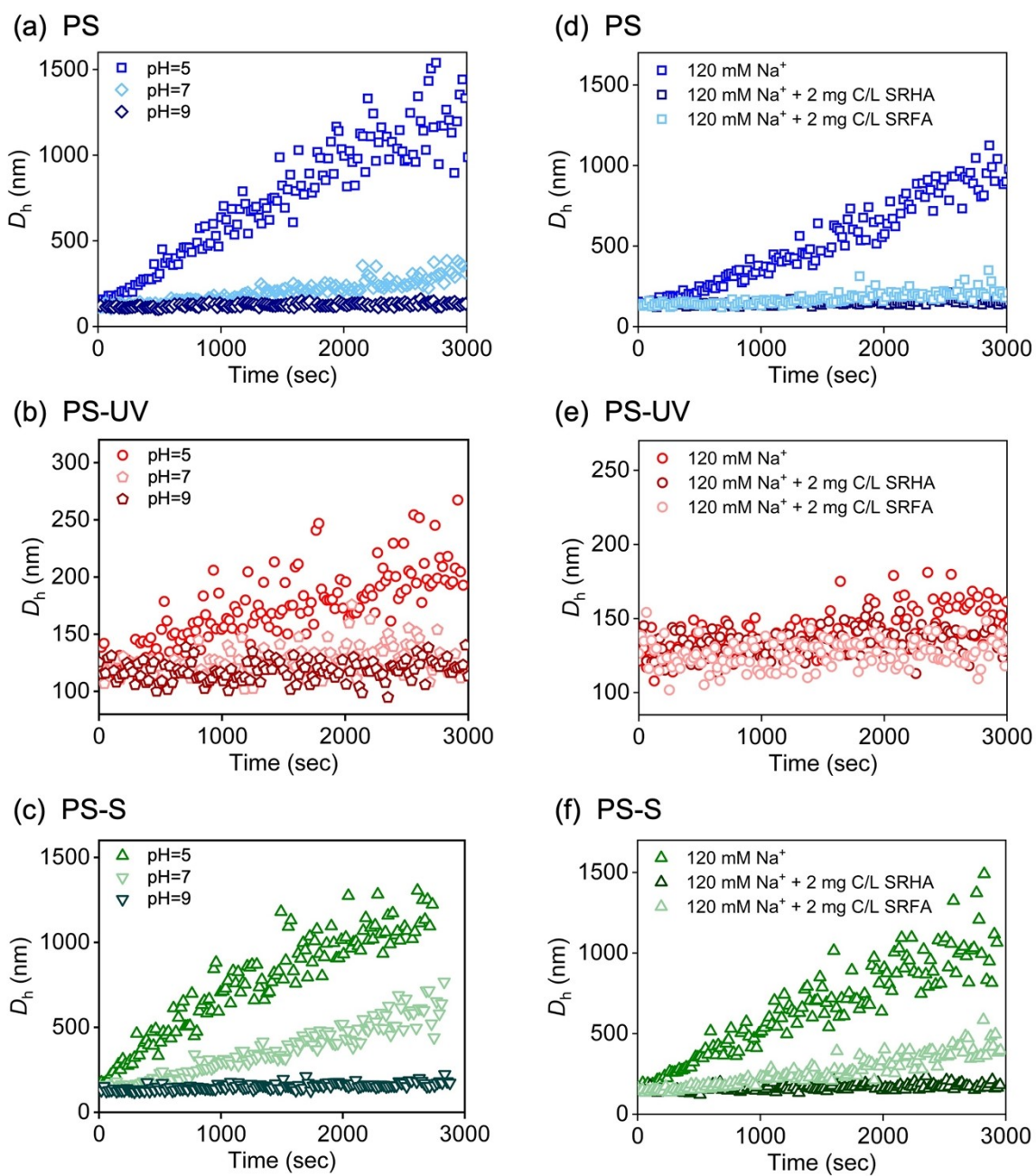


Fig. S4. Aggregation kinetics of PS, PS-UV, and PS-S nanoplastics at different pH conditions (a-c) and in the absence or presence of NOM (d-f).

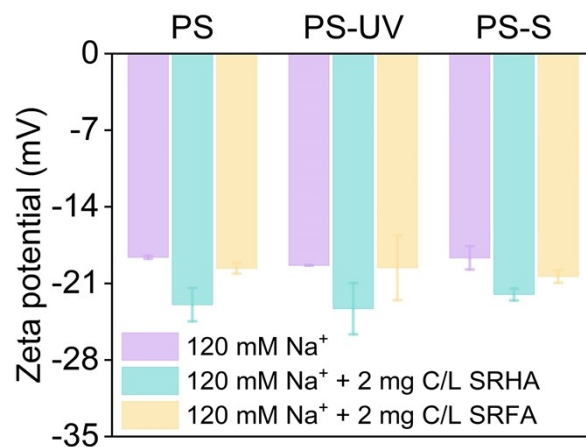


Fig. S5. Zeta potential of PS, PS-UV, and PS-S nanoplastics in the presence of 120 mM NaCl with or without NOM.

References

1. Su, J.; Ruan, J.; Luo, D.; Wang, J.; Huang, Z.; Yang, X.; Zhang, Y.; Zeng, Q.; Li, Y.; Huang, W.; Cui, L.; Chen, C., Differential Photoaging Effects on Colored Nanoplastics in Aquatic Environments: Physicochemical Properties and Aggregation Kinetics. *Environmental Science & Technology* **2023**, *57*, (41), 15656-15666.
2. Zhao, M.; Zhang, T.; Yang, X.; Liu, X.; Zhu, D.; Chen, W., Sulfide induces physical damages and chemical transformation of microplastics via radical oxidation and sulfide addition. *Water Research* **2021**, *197*, 117100.